



JRA1 Delivery: Test Report on the EUDET High Resolution Pixel Telescope

The EUDET JRA1 Group*

December 29, 2008

Abstract

Within the EUDET consortium a high resolution pixel beam telescope is developed. The telescope consists of six planes of monolithic active pixel sensors and can be operated in a magnetic field of 1.2 T. A flexible data acquisition is available for the telescope and the system is equipped with all required infrastructure. Since the first installation of a demonstrator telescope in 2007, it has been extensively tested and used by various detector R&D groups. Results from testbeam measurements to obtain the telescope performance are described here. The sensors of the final telescope will provide digital outputs and zero suppression. This report is a delivery within the JRA1 activity of EUDET (JRA1-D6).

*contact: Ingrid-Maria Gregor, DESY, Hamburg, Germany (ingrid.gregor@desy.de)

Contents

1	Introduction	3
2	Telescope Requirements and Overview	3
3	The Sensors	5
3.1	Reference Plane Sensors - MimoTel	6
3.2	The High Resolution Plane - Mimosa18	7
4	The DAQ system	7
4.1	The Data Reduction Board - EUDRB	8
4.1.1	EUDRB Motherboard	9
4.1.2	EUDRB Digital Daughter Card	10
4.1.3	EUDRB Analog Daughter Card	10
4.2	Trigger Logic Unit	11
4.2.1	Operating Modes	12
4.2.2	Interfaces	12
4.2.3	Handshake with Device Under Test	12
4.3	DAQ Software - EUDAQ	13
4.4	User DAQ Integration	14
5	The offline analysis software - EUTELESCOPE	15
5.1	GRID Installation	17
5.2	Alignment	17
5.2.1	Local and global parameters	18
5.2.2	Constraints	19
5.2.3	Description of the steering files	19
6	Mechanical Setup	19
7	All-inclusive Package for the Telescope User	23
8	Demonstrator Test Beam Results	23
8.1	Characterisation with MiPs	23
8.2	Characterisation with Hadrons	24
9	Test Beam Campaign 2008	24
9.1	SiLC	25
9.2	CALICE	25
9.3	DEPFET	26
9.4	ISIS	26
10	Outlook: Towards the final digital readout	26
11	Summary	26

1 Introduction

A linear electron-positron collider operated at the centre-of-mass energy of at least 500 GeV is the next great international project in high energy physics. The EUDET project which is supported by the EU in the 6th Framework Programme (FP6) aims to provide infrastructures for the R&D of detector technologies towards the international linear collider. Within the EUDET project the JRA1 activity works on the improvement of testbeam infrastructures. For this purpose a high resolution pixel telescope is developed. The design goals include a high position resolution ($\sigma < 3.0 \mu\text{m}$) and readout rate of 1 kHz. Additionally, the telescope can be operated in a 1.2 T solenoid magnet (PCMAG). The construction was planned in two stages, to quickly offer an exploitable infrastructure in parallel to the development of the final telescope. In the first stage (demonstrator telescope) a well established CMOS pixel technology with an analogue readout were used. The analog-to-digital conversion and signal processing is realised using fast processors in the readout electronics. This first telescope does not satisfy the final requirements (see section 2) with respect to chip size. But a first test facility was available quickly to satisfy immediate and urgent test needs of various research groups working on pixel detectors in Europe. Within the first year of operation numerous detector R&D groups used the telescope for their test beam studies at the DESY electron beam and the CERN-SPS hadron beam. In this report the requirements for such a high precision telescope, the construction, and the first exploitation by users will be described. At the end an outlook on the design of the final telescope with a fully digital sensor will be given.

2 Telescope Requirements and Overview

The beam telescope is to be used for a wide range of R&D applications and quite different devices under test (DUT), from small (a few millimetres) to large (up to one meter) size. Depending on the project and on the size of the device the requirements as to precision and coverage are quite different. Still, the system should be easy to use so that a high efficiency in the use of the facility can be achieved.

Due to the limited energy of the electron beam from DESYII (1 – 6 GeV) the precision that can be reached in any device is limited by the multiple scattering. However, with a careful optimisation of the telescope setup with respect to dead materials and positioning of the telescope planes the precision of the predicted impact position of beam particles on the DUT plane should reach less than $3 \mu\text{m}$ at 6 GeV. This is achieved by reducing the amount of material in individual planes while maintaining point precision on the telescope planes of around $2 - 3 \mu\text{m}$. Simulations showed that the insertion of a high resolution plane ($\sigma \approx 1 \mu\text{m}$) in front of the DUT improve the precision of the telescope [9].

The mechanical setup should allow for a wide range of different configurations from a very compact one useful for pixel sensors to a two-arm layout with sufficient adjustable space in between the arms to accommodate a DUT. The lateral dimensions of the active

area should be large enough to cover high precision pixel devices without mechanical movement of the device under test. Mechanical actuators will be used to adjust the DUT position within the telescope or to scan the DUT in case of larger devices. The speed of the device should allow to take full advantage of the beam rates and hence should be able to operate at readout rates of up to 1000 frame/sec. Finally, the overall setup of the telescope should be flexible enough to make it transportable in order to use it at other beam lines outside of DESY, e. g. at higher energy hadron beam lines.

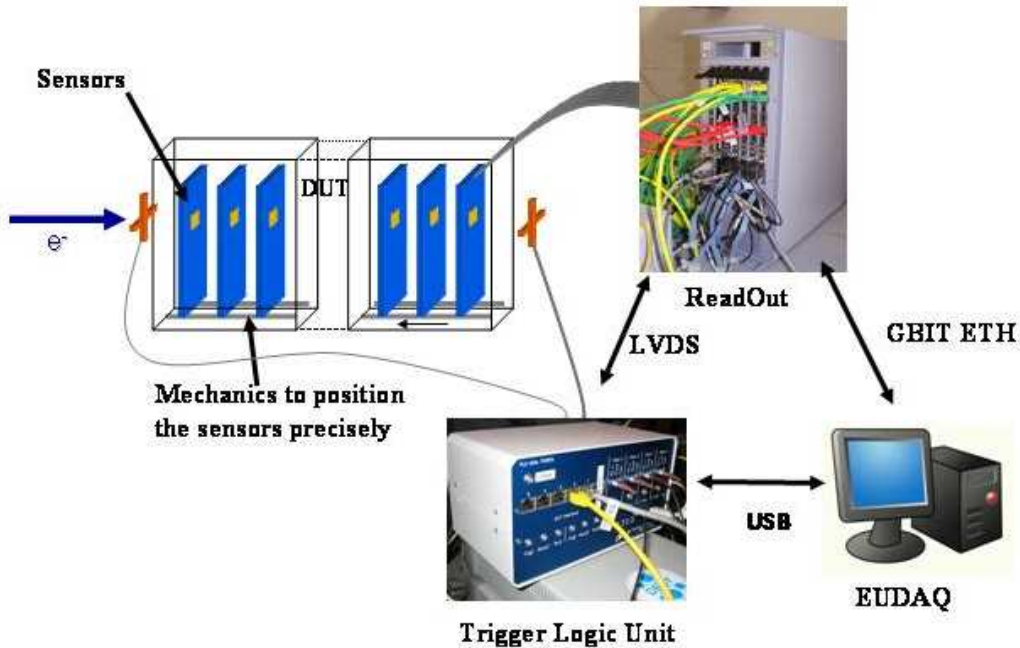


Figure 1: Overview of the components needed for an analogue telescope.

In Figure 1 all "ingredients" for a pixel telescope are shown. In the following sections the availability and status of all these components will be described:

- Pixel sensors with a single point resolution of 2 - 3 μm and a minimum of material.
- Precisely worked mechanics to position the sensor boards in the particle beam.
- The readout boards adapted to the pixel sensors.
- A DAQ system including trigger and software.
- A analysis software for reconstruction, alignment and tracking.

3 The Sensors

The sensors for the telescope have to provide a single point resolution of $2 - 3\mu\text{m}$ with a minimum of material. Also, a reasonable lateral coverage is required and the readout has to be fast enough to reach a telescope frame rate of 1 kHz.

R&D towards an ILC vertex detector is actively being pursued on a number of different sensor technologies such as CCDs [2], DEPFETs [3] and CMOS [4] sensors and a number of prototypes emphasising different aspects of these devices have been built. Most of these prototypes are too small for the planned telescope.

However, the CNRS-IPHC institute in Strasbourg, France [5] has also successfully developed, fabricated and tested a number of monolithic active pixel sensors (MAPS) with large enough arrays for the telescope. The MimoTel prototype, was chosen for the demonstrator telescope. For the high resolution plane the Mimosas18 was developed.

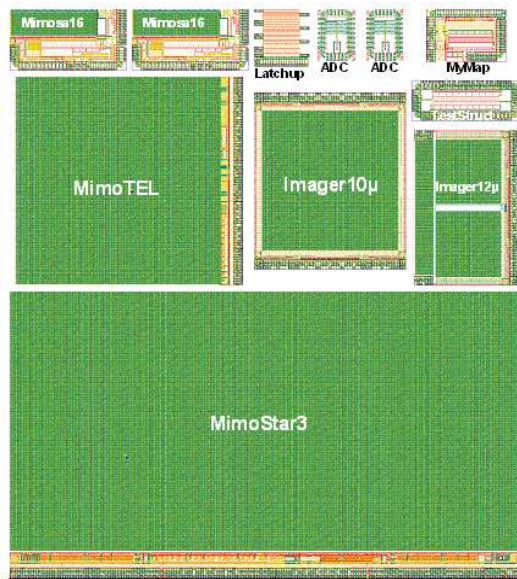


Figure 2: Layout of the reticle of the engineering run AMS-035 OPTO 07/2006 on $14\mu\text{m}$ (standard) and $20\mu\text{m}$ epi substrate

Both sensors were processed in the AMS 0.35 OPTO process. The AMS- $0.35\mu\text{m}$ OPTO process has been chosen for several reasons: It is an advanced mixed-signal CMOS process, providing four metal layers, two polysilicon layers, high-resistivity polysilicon and two types of transistor gates (3.3 V and 5 V). The N-well/p-epi diodes are optimised for a low dark current at room temperature. The feature of a special interest is epitaxial layer having more than $10\mu\text{m}$ thickness. Such a thick epitaxial layer provide a comfortable charge signal from passing minimum ionizing particles. The process is available through multi-project submission runs at Austria Micro Systems (AMS) which allows easy and cheap prototyping [10]. In Figure 3 the layout of the reticle of the engineering run is shown. The engineering run was in summer 2006 and the chips were received October 2006.

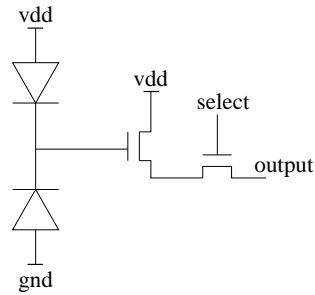


Figure 3: Self biased pixel circuit of the MimoTel and Mimosa18.

	MimoTel	Mimosa18
Pixel Pitch [μm]	$30 \mu\text{m} \times 30 \mu\text{m}$	$10 \mu\text{m} \times 10 \mu\text{m}$
Subarrays	4 of 64×256 pixels	4 of 256×256 pixels
Number of pixels	65536	262144
Active area [$\text{mm} \times \text{mm}$]	7.7×7.7	5×5
S/N		
Intrinsic resolution [μm]		

Table 1: Main parameters of the reference plane sensor MimoTel and the high resolution plane Mimosa18

3.1 Reference Plane Sensors - MimoTel

As sensors for the reference planes the MimoTel prototype is used. This is a chip processed in the AMS 0.35 OPTO process with 14 and $20 \mu\text{m}$ epitaxial layer. It is subdivided into four sub-arrays of 64×256 pixels. The pixel pitch is $30 \times 30 \mu\text{m}^2$ resulting in an active area of $7.7 \text{ mm} \times 7.7 \text{ mm}$.

More Details for MimoTel to be added

3.2 The High Resolution Plane - Mimosal8

Mimosal8 is optimized for high resolution tracking. It consists of 512 x 512 pixels, with a pixel pitch of 10 μm . A continuous tracking sensitive area with this device is of $5 \times 5 \text{mm}^2$. A simple read out architecture consists of a 2-transistor pixel cell (half of a source follower plus a readout selection switch) connected to the charge collecting Nwell diode, continuously biased by another diode (forward biased) implemented inside charge sensing Nwell.

The signal information from each pixel is serialized by a circuit (one per sub-array), which can withstand up to a 25 MHz readout clock frequency. This provides Mimosal8 full frame readout time of 3 ms (with four parallel outputs). In this architecture, the frame readout time is equal to the signal integration window. Information from two consecutive frames was read out: one frame before and one frame after each trigger. A data analysis based on the correlated double sampling (CDS) method was used for hit reconstruction. The high resolution tracker (Mimosal8, called also Imager10 μ) was part of an engineering run submitted by IPHC in June 2006, re-submitted in 2007 and 2008. Figure 3 shows the layout of a single reticle ($2 \times 2 \text{ cm}^2$ silicon area) from this submission, which contains several other sensors including EUDET reference sensor for the demonstrator phase (MimoTEL). Two types of wafers were used for this engineering submission: a standard wafers with 14 m epitaxy and an experimental wafers with 20 μm epitaxy.

4 The DAQ system

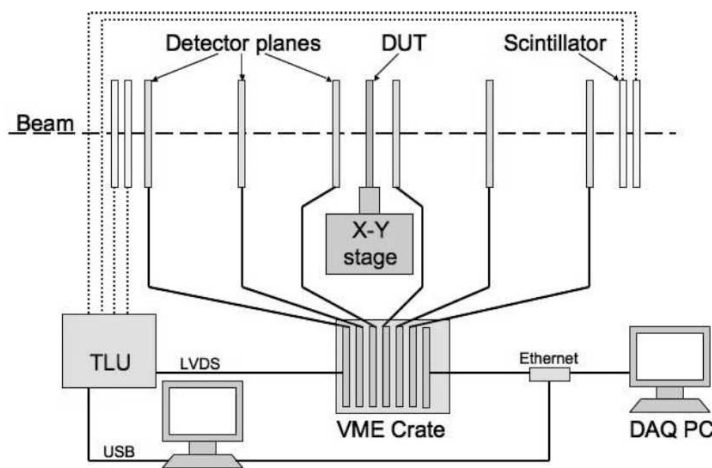


Figure 4: The DAQ system of the EUDET pixel telescope.

The data acquisition system, as shown in Figure 4 for the EUDET beam telescope is a combination of dedicated hardware and software with the following sketched data flow:

The pixel sensors are read out by custom made data reduction boards (EUDET Data Reduction Board - EUDRB), sent via VME64x block transfer to a VME CPU (PowerPC MVME6100) and from there via Gigabit Ethernet to the central DAQ computer. This DAQ computer combines the telescope events with the information from the custom made Trigger Logic Unit (TLU), which is controlled by its own PC. The whole system is controlled by the EUDET Data Acquisition software (EUDAQ). The system allows flexible integration of multiple Devices under Test (DUTs). Offline analysis of the data is performed within the ILC software framework on the GRID using a dedicated EU Telescope package. The details to the different components are given below.

4.1 The Data Reduction Board - EUDRB

The EUDET Data Reduction board (EUDRB) was developed to read out Monolithic Active Pixel Sensors (MAPS). The board generates detector timing signals in LVDS logic levels and provides analog to digital conversion of the four analog single-ended/differential input with 12bits resolution at a sampling frequency currently set at 10 MHz.

The EUDRB also features an output port (with TTL signalling levels) to configure detectors with JTAG programmable features. The motherboard has 4 banks of 256k×48bit SRAM memories providing storage for up to three full frames for a 1Mpixel sensor like the MIMOSA-5. On this collected data the EUDRB performs Correlated Double Sampling (CDS), pedestal subtraction and threshold comparison to reduce the data size for the events selected by the experimental trigger. However, the EUDRB also provides the full frame information when the RAW operating mode is selected. The EUDRB features a 256k×32bit FIFO memory to provide temporary storage for data selected by a trigger and waiting to be readout. Both a VME and a USB2.0 interface are implemented; the EUDRB may be used for reading out the MAPS both in standalone mode on a bench-top and in a standard VME-based data acquisition system. The trigger input port on the front panel of the EUDRB was designed to interface it to the EUDET Trigger Logic Unit (TLU) (see section 4.2) and a trigger bus is also foreseen to distribute/receive trigger information over the free lines of the VME J2 connectors by means of a private bus on flat cable.

Two LEMO connectors on the front panel of the EUDRB can be used to synchronize the data collection operations over a pool of boards. The operation of the EUDRB is controlled by an ALTERA Cyclone II Field Programmable Gate Array (FPGA) device in which a NIOS-II microcontroller is also implemented to do initialization, housekeeping and diagnostic. An 8 MByte serial configuration device EPCS64 is used to store both the FPGA configuration information and the microcontroller code. At power up the FPGA loads its configuration from the EPCS64 and begins operation; the first task executed by the NIOS-II is to copy its ROM-resident code from the EPCS64 to its 1MByte program/data RAM and then jump to executing the code in RAM.

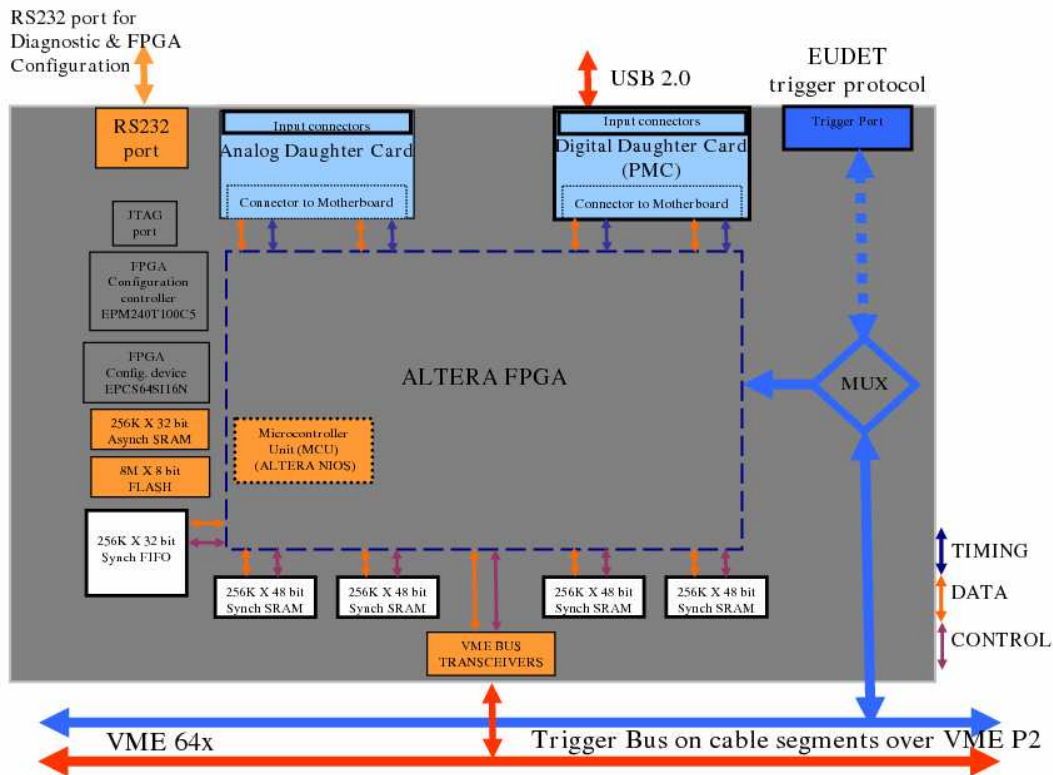


Figure 5: Diagram of the EUDRB functionality.

4.1.1 EUDRB Motherboard

The larger green block represents the motherboard (EUDRB_MoBo) and the resources supported by it:

- the ALTERA EP2C70F896C8 FPGA (dashed blue outline) with the NIOS-II block in evidence. Details of the sequencers and logic blocks implemented in the FPGA are given in a later section
- the four banks of 256k x 48bit SRAM whose function is to hold the pixel voltage samples recorded during the last three scans of the four MAPS submatrices. The SRAM also hold values of pedestal (6bits) and threshold (6bits) which are specific to each pixel
- the 256k x 32bit FIFO used as temporary storage for the data requested with a trigger pending the readout through the VME or USB2.0 port utilities:
- the 256k * 32bit SRAM used as program/data memory by the NIOS-II
- the 1M * 8bit Flash (non volatile) memory which could be used by the NIOS to store permanent data (i.e. default pedestal/threshold values)

- the configuration device EPCS64
- the configuration controller based on an ALTERA EPM240T100 which provides an alternate method for bootstrapping the FPGA
- the EUDET TLU ports: the front panel port to connect the EUDRB directly to the EUDET Trigger Logic Unit. An EUDRB connected to the TLU will act as the TLU-Interface for all the EUDRBs in a VME crate. The TLUInterface fans out the trigger informations to other EUDRBs via a private bus on a cable segment installed on the free pins of the VME P2 connectors
- the RS-232 port which allows a simple and direct connection of the NIOS-II to an host PC for lower level diagnostics and debugging

4.1.2 EUDRB Digital Daughter Card

The EUDRB_DCD is a board with standard PCI Mezzanine Card (PMC) format and PMC compatible connectors toward the EUDRB_MOBO. On the front side of the EUDRB_DCD four connectors are available. The EUDRB_DCD features a Cypress CY7C68013A-56PVXC, which, like in the MAPS readout boards designed by the SUCIMA collaborations, provides a relatively simple way of interfacing the EUDRB's FPGA to an USB2.0 bus, via the front panel connector J4. The CY7C68013A-56PVXC holds its bootstrapping data into a 24LC128 128kbit serial EEPROM. The EUDRB_DCD then provides an I/O port with single ended 3.3V TTL signal levels (connector J1, RJ45) to control the configuration of sensors with features programmable via a JTAG interface, like the IPHC MIMO*2. The J2 connector provides detector timing signals (Scan Clock and Scan Reset) in LVDS format. For driving the MIMOTel sensor used in the demonstrator telescope an interface board has been developed at INFN Ferrara (MIMOTel level adapter) which translates the voltage levels of the JTAG signals from the EUDRB_DCD J1 connector, rearranges connector pin definitions and drives the output signals through two RJ45 connectors to the MIMOTel. Fig. 2.4 shows the electric diagram of the MIMOTel level adapter. The J3 connector receives detector timing signals (Scan Clock and Scan Reset) in LVDS format from an external source (like a sensor's proximity board or another EUDRB). This feature has not been used in the demonstration telescope because a different port, on the analog daughter card) for such synchronization signals has been used.

4.1.3 EUDRB Analog Daughter Card

The EUDRB_DCA is a board with standard PCI Mezzanine Card (PMC) format and a pair of IEEE-1386 PMC connectors toward the EUDRB_MOBO; the signals assignment on this connectors is not compatible with the PMC standard. On the front side of the EUDRB_DCA two RJ45 connectors are available, whose pin definition is reported in Fig. 2.3; there are also 6 LEMO connectors, as shown in Fig. 2.5. The EUDRB_DCA J1 is the port for the differential analog input signals, which are usually buffered and

driven differentially by the sensors proximity board along a four-pair shielded twisted cable, to reduce noise pick-up. The EUDRB_DCA J2 is an output port which could provide four channel of polarization voltages or four static signals to the MIMOSA-5 detector to configure its operating mode. The main task of the EUDRB_DCA is to digitize the four input signals. The design of the ADC stage and its ADC driver is based on the designs developed by the IPHC in Strasbourg and the University of Cracow and exploited by the SUCIMA collaboration. The four A/D converters used on the board are of the type AD9226 by Analog Devices. The AD9226 resolution is 12 bit and its sampling frequency can reach 65MHz. The AD9226's differential inputs (with a 2V dynamic range) are driven by a buffer stage based on the differential amplifier AD8138. The buffer stages also take care of translating the single ended inputs from the LEMO connectors into the differential format; this option can be enabled by modifying solder-jumpers on the analog daughter card.

The two following modes of operation have been implemented in the EUDRB firmware so far:

- **Transparent mode:** All pixel signals are transferred without further data processing. This mode is important for debugging and for the characterisation of the telescope sensors itself.
- **Zero suppressed mode (ZS):** The correlated double sampling (CDS) is performed online and only the signals and addresses of pixels above a certain user-defined threshold are transferred. This mode is intended for datataking at high rates keeping the output files reasonably small.

The output of the EUDRB boards is collected by a MVME6100 single board computer which is located in the same VME64x crate. Finally, the data are send to the main DAQ PC using gigabit ethernet. This computer can also collect the information from the device under test (DUT).

4.2 Trigger Logic Unit

A simple easy to use trigger system is desirable for a user telescope, given that at beam-tests rapid installation of the device under test is often needed. Triggering on beam particles has traditionally been done using modules housed in NIM crates[16]. However, NIM crates are bulky and heavy. Moreover they are either expensive if purchased new or often in poor repair if drawn from a “loan pool”. In addition it is not straightforward to expand a NIM trigger system to provide trigger time-stamping, allowing self-triggered or triggerless operation of the device under test (DUT). Modern field programmable logic allows construction of a low-cost, compact and flexible trigger unit which addresses these issues.

An important design aim was to place few *restrictions* on the user of the TLU, whilst being as flexible as possible. The trigger unit should be as simple as possible, since ILC detectors will not be triggered. It should also be low cost, to allow widespread

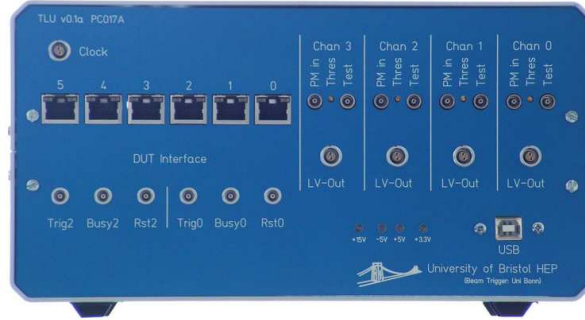


Figure 6: Front Panel of the TLU

distribution. Ideally, each group developing detectors should be able to have at least one TLU.

4.2.1 Operating Modes

The TLU is able to provide “classic” beam-test trigger system. Incoming beam triggers are combined in a user selectable combination and passed to one or more DUT. The TLU also keeps a record of the arrival time of each trigger. Hence it can operate as time-to-digital converter for triggerless or self-triggered DUT. Both modes are active simultaneously, allowing triggered and triggerless/self-triggered DUT to be mixed in the same beam-test.

4.2.2 Interfaces

Four 50Ω terminated coaxial connectors accept NIM, TTL or photo-multiplier level pulses and receive a trigger for each particle passing through the test-beam. These four inputs are combined to form a beam-trigger. The arrival of a beam-trigger will cause a trigger to be output to active DUTs, unless one or more have indicated that they are busy. Interface to the DUT is via RJ45[15] connectors each carrying four LVDS signals. The signals from the TLU to the DUT are *trigger* and *reset*, the signals from the DUT to the TLU are *busy* and *DUT-clock*. There are six DUT connectors.

The FPGA is configured via the USB interface. Memory-mapped communication is used for setup and control. Then, block transfer is used to transfer time-stamps from the TLU to the host computer.

A photograph of the TLU front panel showing the various interfaces is shown in figure 6.

4.2.3 Handshake with Device Under Test

There are three handshake modes available for communication between the TLU and the DUT. The modes can be mixed, with different DUT using different handshake modes. The handshake modes are:

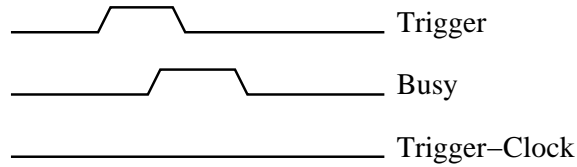


Figure 7: Simple Handshake Mode

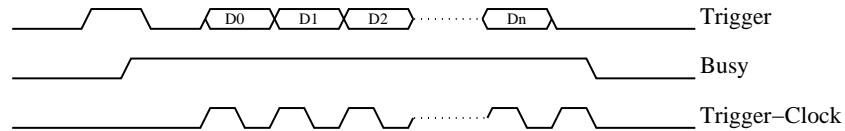


Figure 8: Trigger-Data Handshake Mode

- **No Handshake.** The TLU asserts the *trigger* line for a fixed length of time. The *busy* line from the DUT is not monitored. In this mode the TLU acts like a simple discriminator and coincidence/veto unit.
- **Trigger/Busy Handshake.** The TLU asserts the *trigger* line connected to every DUT in the system. The TLU waits for each DUT to assert its *busy* line. When a DUT does this, the TLU de-asserts the corresponding *trigger* line and waits for the DUT to de-assert its *busy* line. The TLU does not issue any further triggers until all the DUT drop their *busy* lines. This mode is illustrated in figure 7.
- **Trigger/Busy/Trigger-Data Handshake.** This mode is similar to the Trigger/Busy handshake, but trigger information is transferred from the TLU to the DUT. When the TLU de-asserts the *trigger* line in response to the DUT asserting its *busy* line, the DUT toggles its em DUT-clock line and the TLU will clock out trigger information on the *trigger* line. Normally the trigger information is the bottom sixteen bits of the trigger counter. After the DUT is ready for new triggers and has clocked out the trigger information, it de-asserts the *busy* line. This mode is illustrated in figure 8.

4.3 DAQ Software - EUDAQ

The custom DAQ software named EUDAQ has been implemented in C++ [25]. Several producer tasks communicate with a global run control using sockets. These producer tasks connect to the hardware of the beam telescope, to the TLU and eventually to the DUT. Data from all producers is sent to the central data collector and can be monitored by several processes. An online monitor based on the ROOT framework showing online data quality monitoring histograms as well as a process to collect log messages are available. EUDAQ runs on MacOS, Linux and Windows using cygwin.

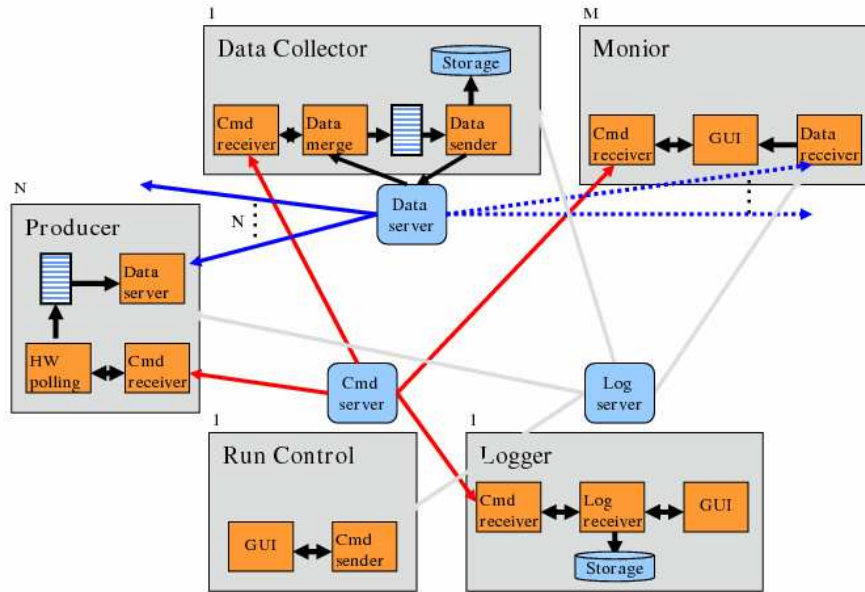


Figure 9: Overview

4.4 User DAQ Integration

Different scenarios for the integration of the DUT in the DAQ system of the EUDET pixel telescope are possible:

- **Integration at hardware level:** In this case the user has to provide a hardware interface able to read out the telescope sensors and the DUT. This approach is supported by the EUDRB boards, but is only feasible for some dedicated DUTs.
- **Integration at DAQ software level:** The user provides own DAQ hardware to read out the DUT, but the data are be treated by a common DAQ software. In case EUDAQ is used as the common DAQ system, a producer to read out the DUT needs to be implemented.
- **Integration at trigger level:** This default scenario was chosen by most users so far, because it is easy to implement and relatively safe. Different hardware and software are used for the telescope and the DUT. The synchronisation is done using the trigger, busy and reset logic provided by the TLU. To protect against slippage of event numbers between the telescope and the DUT, the event number provided by the TLU can be read by the DUT.
- **Integration at data level:** Both, the DUT and the telescope use their own dedicated DAQ hardware and software. The data streams are combined offline by inter process communication. In this scenario the synchronisation and the configuration during the start-up might be difficult.

5 The offline analysis software - EUNETElescope

For the offline reconstruction of track positions in the DUT the software package EUNETElescope has been developed which is implemented as a set of Marlin processors [26]. This design allows to integrate the DUT data at different steps of the analysis chain. Furthermore, the package is prepared to be executed on the Grid to allow a fast processing of large datasets.

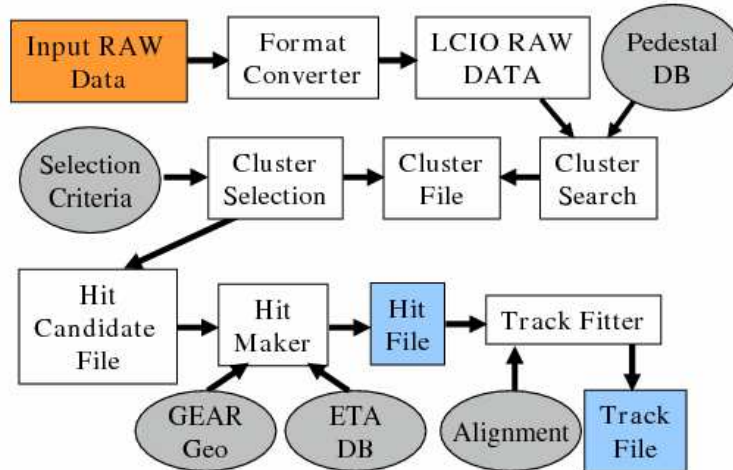


Figure 10: Schematic overview of the offline analysis package EUNETElescope.

Figure 10 summarises the structure of the offline analysis package. Each step in the analysis procedure is implemented in a separate Marlin processor. It is possible to run each processor separately or to execute the whole analysis chain by a single command. In the first step the data is converted from a native format used by the EUNDAQ software to the LCIO format. Afterwards a pedestal correction is applied and clusters are searched for. It is possible to improve the reconstructed cluster positions using the η algorithm. Clusters are accordingly transformed into hits in the telescope frame of reference. The alignment procedure is based on the Millepede II package and uses full tracks in a simultaneous fit to derive the alignment parameters. Finally, tracks are fitted using the hits after the alignment constants have been applied. The result of the track fit can be saved in a ROOT file if needed by the user of the telescope. One design aspect was to benefit as much as possible from the existing ILC software framework which is described elsewhere [29].

The different steps of the analysis chain within EUNETelescope are performed by dedicated processors. A schematic view is shown in figure ???. First, the raw data recorded by the DAQ system are converted to the LCIO format. At the beginning of the development it was decided to have the data acquisition system writing the acquired data directly in LCIO [?] format, but even if a feasibility test proven that this was possible, both the DAQ and the analysis experts decided to keep a very simple platform and system independent

native format that can be decoded also by users not using the ILCSOFT infrastructure. This native data format is promptly converted into the LCIO data collections used by EUTelescope to perform all the analysis steps. Afterwards clusters are searched for and cuts are applied to the cluster candidates. The clusters are transferred to the telescope frame of reference. Now the clusters are referred to as hits.

- **EUTelNativeReader** For this purpose the EUTelNativeReader processor has been coded with the aim of converting all the sub events found within the input native data stream. In this way, an external user, willing to use EUTelescope for his own analysis, has just to write a little excerpt of this universal reader specifying how his detector data should be decoded from the native stream and re-encoded into the LCIO data model. The idea behind this reader is the universal replacement for the EUTelMimoTelReader that was focused on the conversion of events containing only Mimotel sensors and finally also Mimosa18. The EUTelNativeReader will guess from the Beginning Of Run Event (BORE) which kind of sensors are present in the telescope setup and fill in a list of EUTelBaseDetector derived classes, each of them is implementing a precise sensor configuration. For each group of sensors there will be a common output collection containing the raw data information.
- **EUTelCorrelator** This is a very useful diagnostic tool that users can use to understand if the data quality is acceptable and if the geometry description they provided is effectively compliant with the reality. EUTelCorrelator is taking as input either a collection of clusters (group of pixels on the same sensor) or a collection of hits (space points in the global telescope frame of reference) and filling series of two dimensional plots showing the correlation of the cluster / hit position with respect to all other cluster / hit not belonging to the same plane.
- **EUTelMAPSDigi** This was the last piece of code needed to make our software a complete suite for analysis and reconstruction. EUTelMAPSDigi is digitization processor. A realistic model based on the beam test results is used to calculate the expected response of MAPS sensors for the Geant4 simulated hits, as returned by Mokka. The conversion from global reference frame to local reference frame of individual sensor, based on the GEAR geometry description, was adopted from EUTelHitMaker. Each Mokka hit is divided into a number of smaller steps (based on energy deposit and path length). For each step corresponding charge deposit in sensor pixels is calculated by 2D integration of the expected charge density over the pixel surface. Charge capture in silicon (signal attenuation) and charge reflection from the epitaxial layer boundary are also taken into account. The core of the algorithm is implemented in TDS (Track Detailed Simulation) package by Piotr Niezurawski (pniez@fuw.edu.pl). With this new processor, users can simulate realistic reference data sample and estimate their DUT figures of merit before collecting real test beam data.

- **EUTelPedestalNoiseProcessor** This processor has been revisited to comply with some specific user requests, like the possibility to perform a Common Mode rejection on a row wise base instead of full sensor and different dead / noisy / hot pixels rejection algorithms. These new features are now available to the user community.
- **Histogramming package** This is not really a Marlin processor but a very useful set of ROOT4 macros opening the histogram files produced by the EUTelescope processors and showing relevant histograms and profiles making the data quality monitor much simpler and more effective.

5.1 GRID Installation

The EUTelescope software, being part of the ILCSoft, has been installed on the Experiment Software Area of all the Computing Elements accepting job submission by ILC VO members. In this way, users with a limited knowledge and experience of the GRID can perform their analysis using EUTelescope in a very simple way being all the needed libraries already installed and tested on the target working node. The developers are also thinking of preparing a submission script running standard analysis steps either on the local computer or, if needed, directly on the GRID exploiting parallel processing. his new installation has been used to carry on all the analyses done on the summer 2008 test beam campaign.

5.2 Alignment

Before tracks can be fitted using the hits, the alignment corrections have to be determined. These corrections are needed, because the positions of the sensors in the actual telescope are not identical to the ideal sensor positions in the geometry description. The alignment corrections are given by a set of constants (e.g. shifts and rotations of the sensors) and are passed to the track fitter. Here the structure of the new alignment procedure is explained. A schematic overview is presented in figure 11. Starting point of the alignment is a LCIO file containing information about the positions of the reconstructed hits in the telescope frame of reference.

The Marlin processor **EUTelMille** loops over all desired events. A steering file contains the parameters for the EUTelMille processor, e.g. which constants should be considered. The ideal positions of the telescope sensors are provided by GEAR¹ [30]. Hence a GEAR file has to be specified in the steering file. This GEAR file contains all relevant information about the telescope setup. The EUTelMille processor uses the class **Mille** which is part of the Millepede II package [31]. The class Mille was added to the MarlinUtil [32] program in version v00-05. Hence at least this version of MarlinUtil is required for the alignment.

¹GEometry Api for Reconstructiuon

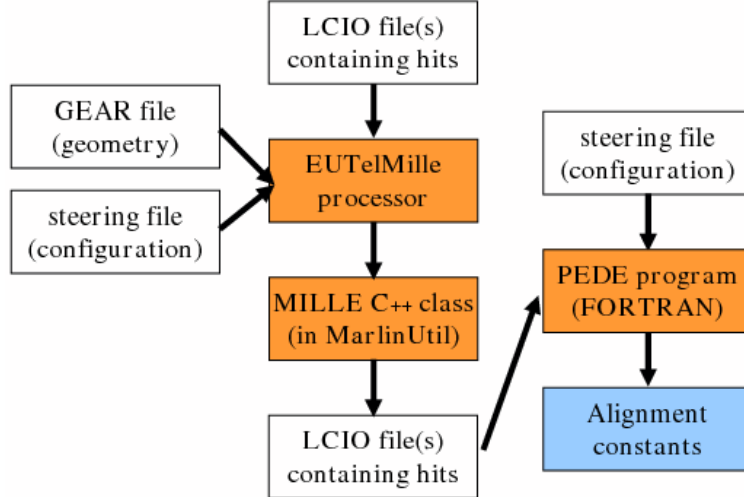


Figure 11: Schematic overview of the new alignment procedure. Data files are represented by green boxes, configuration files are shown as yellow boxes and program code is represented by red boxes. A light blue box shows the resulting alignment constants.

The output of the EUTelMille processor is a C++ binary file. It contains all relevant information needed to perform the alignment fit which is implemented in the **pede** program. Pede was written in Fortran by V. Blobel and performs the least squares minimisation to derive the alignment constants. A further steering file is needed to control the execution of the pede program.

5.2.1 Local and global parameters

In the alignment procedure described here full tracks are used. For this purpose the parameters of the problem are grouped into two classes:

- **Local parameters:** These parameters are only present in a subset of the data. Here the local parameters are given by the parameters describing individual tracks. For the linear track model used the number of local parameters is given by:

$$N_{loc} = 4 \times \text{Number of tracks.} \quad (1)$$

- **Global parameters:** The global parameters are given by the shifts and rotations of the telescope sensors. Hence the number of global parameters is given by:

$$N_{glob} = \text{Number of sensors} \times \text{Number of shifts and rotations.} \quad (2)$$

The pede program solves the linear least squares problem with a simultaneous fit of all global and local parameters, irrespectively of the number of local paramters. The EUTelMille processor has been prepared for the following two scenarios so far:

- All planes can be shifted in the X and Y direction. The parameters are called: $x_0(1)..x_0(N_{sens}), y_0(1)..y_0(N_{sens})$ where the number of sensors is given my N_{sens} .
- Additionallty a rotation around the beam direction is considered: $\gamma_0(1).. \gamma_0(N_{sens})$.

5.2.2 Constraints

To obtain stable results, it is necessary to define constraints. Since this can be done in the pede steering file, the processor EUTelMille does not need to be rerun when the constraints change. One obvious choice of the constraints is to fix the global parameters of two sensors to zero. Usually it is the best choice to fix the first and the last sensor.

An alternative is to fix only the global parameters of one sensor and use additional constraint equations like these:

$$\sum_{i=1}^{N_{sens}} \frac{x_0(i)}{z(0) - z(i)} = 0, \text{ and} \quad (3)$$

$$\sum_{i=1}^{N_{sens}} \frac{y_0(i)}{z(0) - z(i)} = 0. \quad (4)$$

Here $z(1)..z(N_{sens})$ is the number of sensors in the alignment fit.

5.2.3 Description of the steering files

Here all parameters of the Marlin processor EUTelMille and of the pede program are explained in detail. Hence this section can act as a reference for the user.

6 Mechanical Setup

It is foreseen that the beam telescope will be operated in widely varying R&D applications with very different devices under test (DUTs). Four telescope parameters are particularly relevant in this context: the number of measurement planes, the active area, longitudinal size and layout of the telescope, the mechanical support for the DUT and the environmental conditions such as temperature.

Based on detailed analytical calculations [9] it was decided to provide six telescope planes, also for redundancy and flexibility. The telescope will be subdivided into two arms of each 3 sensors to allow more flexibility without limiting the size of the DUT which will be located between the two arms.

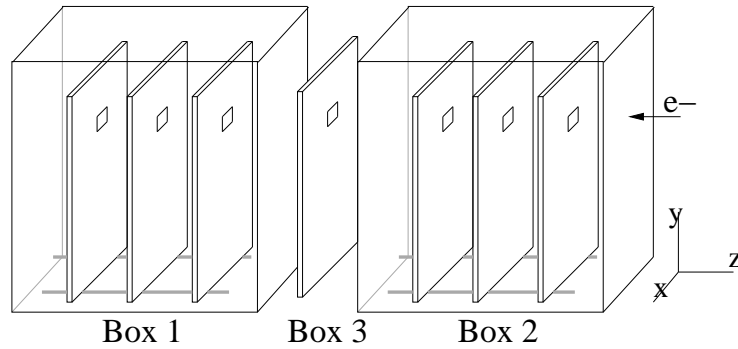


Figure 12: Mechanical concept with three separate areas for the two reference arms and the DUT.

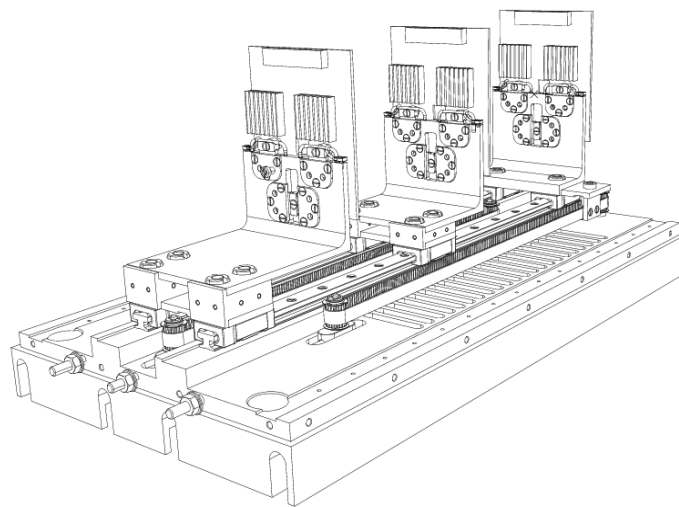


Figure 13: Technical drawing of one arm of the telescope mechanics.

In Figure 12 the mechanical concept for the telescope is illustrated. Three "boxes" will be the main elements. Box 1 on the left side in the illustration is in a fixed position, an "optical" bench within the box guides the three reference planes of the arm in front of the DUT. The box is temperature controlled. Box 2 is movable in z -direction to ease the installation of the DUT as well as to give the possibility of larger DUT devices. The third "box" is the space between the boxes 1 and 2. A cover over this gap ensures thermal enclosure, but this is up to the telescope user. In this illustration the beam is impinging from the right side. For large DUTs mechanical actuation is foreseen in order to move the device through the active area of the telescope.

In Figure 13 the inner mechanical concept of one telescope arm is illustrated. Three sensor jigs (L-piece) are positioned on a track system. For each of the three positions of one telescope arm a different L-piece was designed to allow a minimal distance of x mm between sensor planes. The track system which guides the L-pieces allows a

maximum distance of 200 mm between the outer planes. The distance between the planes is adjustable using a tool from above.

The lower supporting frame is connected to a cooling device (see section ??). The sensors are kept in position on the L-pieces by a clamping mechanism. This design was chosen as high mechanical accuracy was expected. Figure 14 shows a photograph of the inner track system holding one of the L-pieces. A drawing of the complete setup as it was

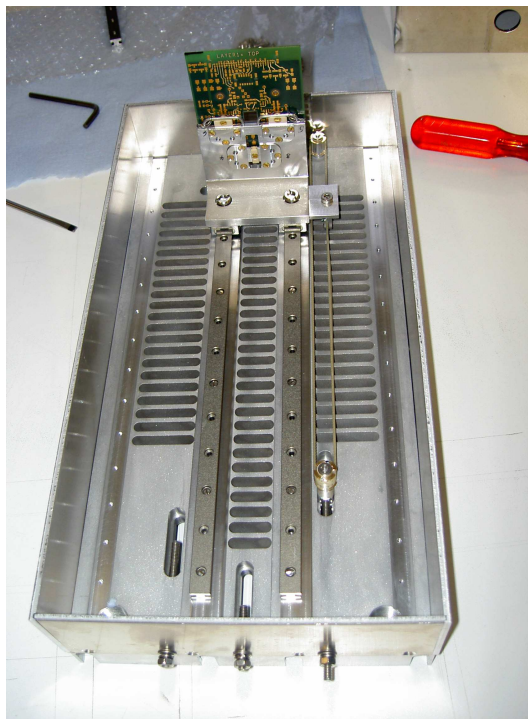


Figure 14: A picture of the actual implementation.

prepared for the CERN test beam is shown in Figure 15. Box 1 and 2 were positioned on a support table built out of a modular system of construction profiles². This allows an easy modification for future different mechanical needs. Each L-piece track system is enclosed by an aluminium lid keeping the sensors in a light tight volume with constant temperature. Special openings for cable feed throughs to the AUX board are foreseen as well as openings for the beam passage covered by a 30um thin aluminium foil. On top of the lids mechanical support for the auxiliary (AUX) boards are located. The gap between box 1 and 2 (box 3) houses a precisely machined platform with fittings for a XY table. All support legs of the table are adjustable in height. A photograph of the setup installed at CERN H8 test beam is shown in Figure 16.

To be added ... The first part of the data was taken at DESY in August 2007 using a compact setup of the telescope where 5 MimoTELS were mounted in a distance of 2.5 cm. Further studies were performed in September 2007 at CERN. Here the sensors

²Rose and Krieger

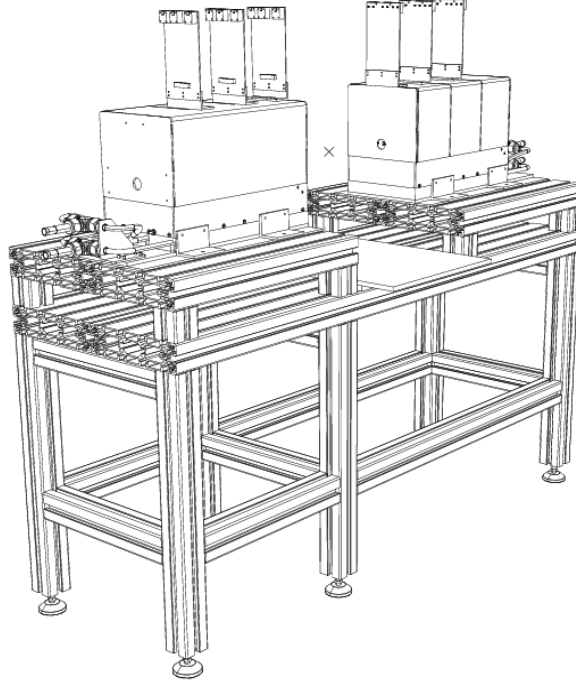


Figure 15: The complete mechanical setup for the CERN test beam.**OLD drawing**

were mounted in two separate boxes with a gap of 34 cm for a DUT in the middle. The first box contained 3 sensors while only 2 sensors were located in the second box. Within the boxes, the sensors were mounted in a distance of 10 cm.

Typically the sensors are shifted by a few hundred μm in the directions perpendicular to the beam and rotated a few mrad around the beam direction. As an example table 2 illustrates the result of the alignment procedure for data taken using a beam of 3 GeV electrons at DESY. Tracks were fitted using the constants provided by the alignment procedure. The mean values of Gaussian functions fitted to the observed residuals in the individual planes are shown. For a perfectly aligned telescope these mean values should vanish. The results demonstrate that the alignment of the telescope is possible with sufficient precision for the intended applications.

Sensor	Mean X [μm]	Mean Y [μm]
0	-0.003 ± 0.002	-0.023 ± 0.002
1	-0.012 ± 0.004	0.036 ± 0.005
2	0.032 ± 0.004	0.005 ± 0.005
3	-0.020 ± 0.004	-0.005 ± 0.005
4	0.001 ± 0.002	-0.002 ± 0.002

Table 2: Mean values of the residual distributions for tracks fitted after the alignment.

7 All-inclusive Package for the Telescope User

After more than one year of user implementation for the telescope we have a complete package to offer to the users:

- The two arm telescope with different geometries with the possibility to add one extra high resolution sensor plane. The telescope comes with all the mechanics and the cooling system for the reference sensors.
- Operating support: mainly remote but also local in some circumstances.
- The DAQ system, both hardware and software. The user can connect the DUT to the EUDET TLU, or (better) help is provided to integrate the DUT R/O in the DAQ software.
- The analysis and reconstruction software EUTELESCOPE. As for the DAQ, the user can rely on the output track file, or integrate the DUT data in the main analysis stream.

The experience with the users in the first two years of running will be summarised in Section 9.

8 Demonstrator Test Beam Results

In this section results from testbeam measurements to characterise the demonstrator telescope are discussed. The demonstrator was commissioned in summer 2007 and tested at test beam at DESY and CERN.

8.1 Characterisation with MiPs

In the setup at CERN two different types of MimoTEL sensors have been used, one kind with a 14 μm thick epitaxial layer and another version had 20 μm thick epitaxial layers. Table 3 shows the signals in ADC counts and the signal to noise ratios for seed pixels and for clusters consisting of 3×3 pixels. The given values represent the most probable value of Landau fits. During the data was taken the telescope was operated using only moderate cooling keeping the sensors at a constant temperature between 20 and 22 degrees Celsius.

For both types of sensors the same amount of charge is collected in the seed pixels. The sensor 3 shows a lower signal to noise ratio compared to the other sensors. This is caused by the fact that sensor 3 has a 20% larger mean single pixel noise which was introduced by the used acquisition and sampling electronics.

In the sensors with thicker epitaxial layers more charge is collected in clusters of 3×3 pixels. This indicates a greater signal production but also a larger charge spread in these sensors compared to the sensors with a 14 μm epitaxial layer. For both sensor types the mean cluster size is around 8 pixels if a threshold of 2.5 times the pixel noise is applied.

If the influence of the telescope material can not be neglected, the resolution can be improved taking the contribution from multiple scattering into account in an analytical fitting approach [13]. Results are shown in Figure 17. The widths of the residual distributions measured in the 5 telescope sensors are shown. The actual plane was excluded from the track fit. Results for beams of 3 and 6 GeV electrons are in agreement with the expectation and with a simulation based on Geant4. In both cases a position resolution of the sensors of $3.0 \mu\text{m}$ was assumed. This demonstrates that a good telescope performance can be achieved even at beam energies of a few GeV.

8.2 Characterisation with Hadrons

If multiple scattering can be neglected, it is possible to fit linear tracks. This is the case for the data recorded using a beam of 180 GeV hadrons in September 2007 at CERN. The X and Y coordinates were fitted separately. The resulting track candidates were required fulfill a cut on $\chi^2 < 20$ in both directions. More than one track candidate per event was allowed. Figure 18 shows the residuals of the tracks in the middle out of 5 sensor planes. Here the middle telescope sensor acts as DUT while the other planes are used to predict the track positions in the DUT. The observed width is consistent with the expectation for the given telescope geometry assuming a position resolution of $3.0 \mu\text{m}$ for the DUT as well as for the other sensors used to fit tracks. Also measurements at DESY using 3 and 6 GeV electrons based on an extrapolation to infinite energy are in agreement with this sensor resolution.

9 Test Beam Campaign 2008

In table 4 the different periods at the CERN test beam and the users of the telescope are listed.

Sensor	Epi thickness	Seed pixel		3×3 Cluster	
		ADC	S/N	ADC	S/N
0	14 μm	47.2	12.5	131.0	11.2
1		46.2	12.2	129.0	10.9
2		47.3	12.8	130.3	11.3
3	20 μm	47.5	10.9	151.4	11.0
4		46.3	12.6	147.6	13.2

Table 3: Signals in ADC counts and signal to noise ratios for seed pixels and 3×3 clusters in the individual planes measured with the setup used at CERN in September 2007. *to be updated to electrons instead of ADC counts AND to new data from DESY Dec 2008*

Table 4: Data collected with EUDET telescope at CERN in summer 2008.

Date	Beam	User	#Runs	#Events
05/08	CERN SPS	SiLC	230	1458173
07/08	CERN PS	CALICE	212	318437
07/08	CERN PS	DEPFET	64	420621
08/08	CERN SPS	MimoRoma	17	23985
08/08	CERN SPS	DEPFET	355	2333133
08/08	CERN SPS	ISIS	427	637866
09/08	CERN SPS	EUDET JRA1	148	342708

9.1 SiLC

In order to build a high resolution silicon strip sensors the strip geometry is of crucial importance. The geometry influences the strip capacity and the charge sharing ability of the strips, both basic properties that contribute to the spatial resolution. Therefore the aim of the project was to evaluate the best strip geometry of silicon strip sensors with 50 microns pitch to achieve the highest possible spatial resolution. For this purpose a custom multi geometry sensor was designed by the SiLC collaboration. Over the 16 zones of this sensor we varied the strip width from 5 to 25 microns. The number of intermediate strips varied between zero and two. The main goal of the test beam was to record data that allows us to estimate the resolution for different detector geometries with the help of the EUDET Telescope. Unfortunately the Telescope's sensitive area, which is $7 \times 7 \text{ mm}^2$ didn't cover the full sensor width of the DUT, so it was necessary to split each measurement into three runs. Each of this resolution runs had 105 events. The different areas on the sensor, covered during the runs, can be seen in the picture on the left. The SiLC group collected about 1.5M events in several configurations with the EUDET telescope. At the time of the annual report the analysis of this data just started. A more advanced report can be found here [?].

9.2 CALICE

One of the aims of the test beam organized by the DHCAL group of the calice collaboration at CERN in July 2008 is the study of the glass resistive plate chamber (GRPC). The latter is a good candidate as a sensitive medium for the high granularity digital hadronic calorimeter proposed for the future International Linear Colliders. The longitudinal granularity of such DHCAL is determined by the size of the electronics board cells used to readout the signal left by the passage of charged particles in the GRPC's gap filled by a special gas mixture. The cell size in the proposed DHCAL is 1 cm^2 . Two cells are separated by a distance of 500 microns. In the avalanche mode regime, the GRPC efficiency depends on the high voltage applied on the two glass plates. For very thin GRPCs as the ones proposed for the DHCAL, the efficiency can be as high as 96% for certain high voltage values. Part of the inefficiency of the GRPCs can be related to

the spacers used to separate the two glass plates. Others inefficiency sources can be the deformation of the electric field on the detector edges and the non-sensitive inter-pad area.

The use of the EUDET telescope in association with the DHCAL setup was a powerful tool to scrutinize the behaviour of the GRPC detector. The precision the EUDET telescope provides has helped to detect an edge effect that one has to solve in order to guarantee a very good efficiency all over the detector. It confirms that the choice of inter-pad distance of 500μ is a good choice to prevent a possible inefficiency.

9.3 DEPFET

The DEPFET collaboration used the EUDET telescope at two different beams at CERN in summ 2998, PS and SPS. At PS they efficiently worked on all little details for the user integration. This was done in the framework of the evaluation of the telescope. At SPS the main goal of the DEPFET group was the measurement of efficiency, purity and intrinsic resolution. The DEPFET was included on DAQ level as described in section ??, meaning that they had their own producer within EUDAQ and only one data stream. One million events were taken while DEPFET was the EUDET DUT. A detailed report on this work can be found here [?].

9.4 ISIS

The charge collection efficiency, charge sharing, hit-efficiency as function of position Standard and the "p-well variant" of ISIS was tested. The analysis of the data is still ongoing.

10 Outlook: Towards the final digital readout

The main difference between the demonstrator and the final telescope which will be assembled and tested starting in spring 2009 is the new sensor called Mimosa 26. This chip consists of 1152 columns of 576 pixels. With a pitch of $18.4 \mu\text{m}$ the Mimosa 26 has an active area of $21.2 \times 10.6 \text{ cm}^2$, which is a factor of 3.8 larger than the MimoTEL of the demonstrator telescope. The integration time of about $110 \mu\text{s}$ allows to read out about 10^4 frames per second. The sensor provides binary output and is equipped with a zero suppression micro-circuit. To reduce the influence of multiple scattering, the Mimosa 26 will be thinned.

11 Summary

The demonstrator telescope is running successfully during several testbeam measurements since about one year. Modularity was one of the most important design aspects for the DAQ hardware and software as well as for the offline analysis package. The analysis of testbeam data shows that the performance of the demonstrator fulfills the

expectations. An increased active area and zero suppression on the sensors will be offered by the final telescope. Interested groups are welcome to contact the EUDET consortium for the exploitation of the device.

Acknowledgement

This work is supported by the Commission of the European Communities under the 6th Framework Programme "Structuring the European Research Area", contract number RII3-026126.

References

- [1] A. Bulgheroni, EUDET-Report-2007-06 (2007).
- [2] K. D. Stefanov, "CCD Vertex Detector for the Future Linear Collider", Nucl. Instrum. Meth. A **501** (2003) 245.
- [3] P. Fischer, W. Neeser, M. Trimpl, J. Ulrici, N. Wermes, "Readout concepts for DEPFET pixel arrays", Nucl. Instrum. Meth. A **512** (2003) 318.
- [4] R. Turchetta et al., "A monolithic active pixel sensor for charged particle tracking and imaging using standard VLSI CMOS technology", Nucl. Instrum. Meth. A **458** (2001) 677.
- [5] Y. Gornushkin et al., "Tracking performance and radiation tolerance of monolithic active pixel sensors", Nucl. Instrum. Meth. A **512** (2003) 299.
- [6] H.S. Matis et al., IEEE Trans. on Nucl. Sci. 50 (2003) 1020.
- [7] Austriamicrosystems, Application Note AMS 0.35 OPTO, <http://www.austriamicrosystems.com/05foundry/indexc35.htm>
- [8] D. Contarato et al., "Beam-test of CMOS pixel sensors with 6 GeV electrons", Proc. Conf. Pixel 2005, to be publ.
A. Gay et al., "High-Resolution CMOS Sensors for a Vertex Detector at the Linear Collider", Nucl. Instrum. Meth. A **549** (2005) 99.
- [9] A.F. Zarnecki, Telescope Resolution Studies, EUDET Annual Meeting, Munich, October 2006
- [10] W. Dulinski, TAPI: high Precision Beam Telescope based on Mimosal8 Monolithic Pixel Sensor and TNT2 Data Acquisition Boards, EUDET-Memo-2008-22, November 2008
- [11] L. Reuen, EUDET-Memo-2007-40 (2007).

- [12] T. Klimkovich, EUDET-Memo-2007-06 (2007).
- [13] A.F. Zarnecki and P. Niezurawski, EUDET-Memo-2007-01, arXiv:physics/0703058v1 (2007).
- [14] A. Cotta Ramusino, EUDET-Memo-2007-36 (2007).
- [15] Telephone terminal equipment - Technical requirements for connection of terminal equipment to the telephone network. Telecommunications Industry Association (TIA) report, ANSI/TIA-968-A, 2002.
- [16] Standard NIM Instrumentation System. U.S. NIM Committee, U.S. Department of Energy Report, DOE/ER-0457T, 1990.
- [17] The ZestSC1 USB FPGA Board. Orange Tree Technologies Ltd Harwell Innovation Centre, 173 Curie Avenue, Didcot, OX11 0QG, UK, 2006.
- [18] EZ-USB FX2LP(TM) - Low Power (Bus Powered) Programmable MCU for bus power peripherals. Cypress Inc, 198 Champion Ct. San Jose, CA 95134 USA, 2006.
- [19] Spartan-3 FPGA Family Data Sheet DS099. Xilinx Inc, 2100 Logic Drive San Jose, CA 95124-3400, USA, 2006.
- [20] ISE WebPACK 9.2i, Xilinx Inc.
- [21] Description of the JRA1 Trigger Logic Unit (TLU). D. Cussans, EUDET-Memo-2007-02, 2007.
- [22] The Design of a Flexible Global Calorimeter Trigger System for the Compact Muon Solenoid Experiment, J. J. Brooke, D. G. Cussans, R. J. E. Frazier, S. B. Galagedera, G. P. Heath, B. J. Huckvale, S. J. Nash, D. M. Newbold, A. A. Shah. Manuscript submitted for publication in Journal of Instrumentation, 2007.
- [23] D. Cussans, EUDET-Memo-2007-02 (2007).
- [24] D. Haas, Proc. of the LCWS'07, Hamburg, EUDET-Report-2007-08 (2007).
- [25] E. Corrin, D. Haas and M. Pohl, EUDET-Memo-2006-07 (2006).
- [26] A. Bulgheroni, T. Klimkovich, P. Roloff and A.F. Zarnecki, EUDET-Memo-2007-20 (2007).
- [27] A. Bulgheroni: *First Test Beam Results from the EUDET Pixel Telescope*, EUDET-Report-2007-06 (2007).
- [28] A. Bulgheroni, T. Klimkovich, P. Roloff, A. F. Zarnecki: *EUTelescope: tracking software*, EUDET-Memo-2007-20 (2007).
- [29] F. Gaede, J. Engels: *Marlin et al - A Software Framework for ILC detector R&D*, EUDET-Report-2007-11 (2007).

- [30] http://ilcsoft.desy.de/portal/software_packages/gear.
- [31] V. Blobel: *Millepede II - Linear Least Squares Fits with a Large Number of Parameters*, draft, available here: <http://www.desy.de/blobel/mptalks.html> (2007).
- [32] http://ilcsoft.desy.de/portal/software_packages/marlinutil.

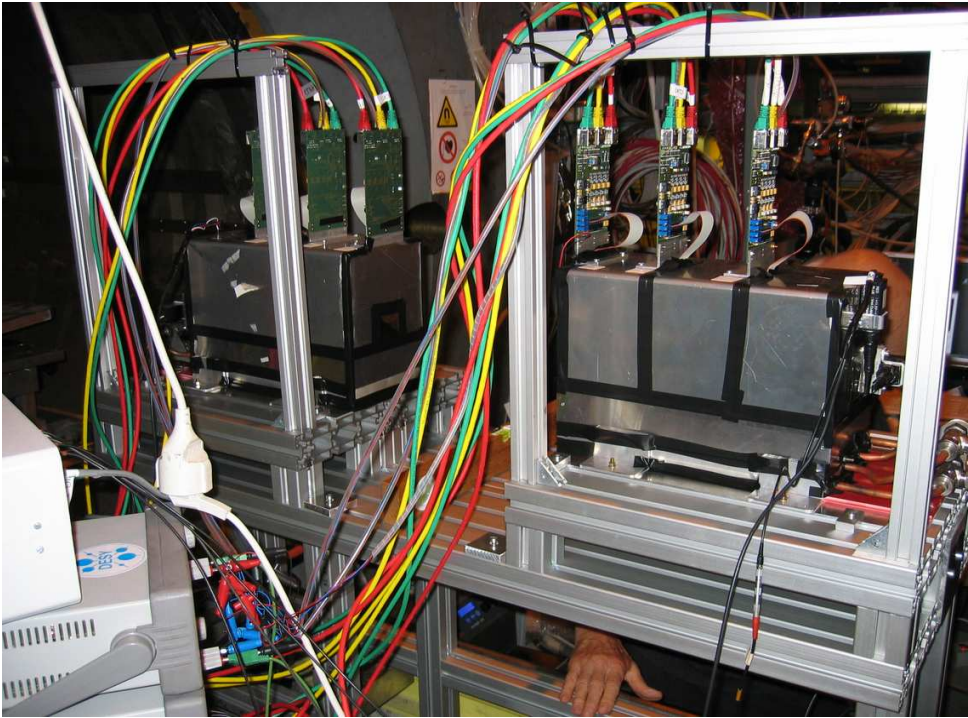


Figure 16: Photograph of the mechanical setup installed at CERN H8 test beam. **OLD photograph**

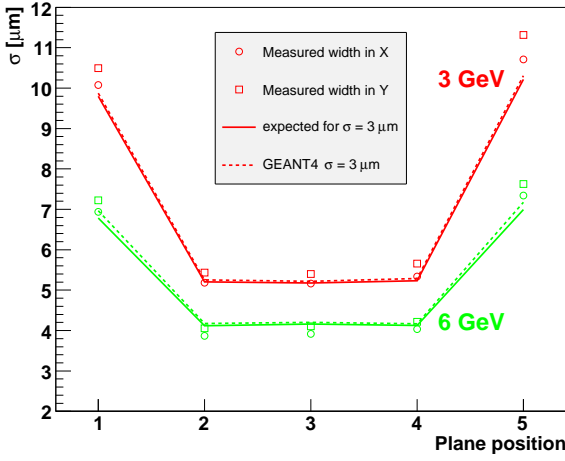


Figure 17: Widths of the residuals in different telescope planes.

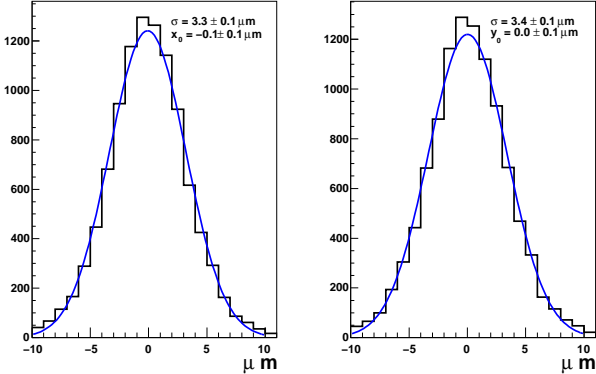


Figure 18: Residuals in the middle telescope sensor in the X (left) and Y (right) directions. This sensor was excluded from the track fit and hence acts as DUT.